Optica Applicata, Vol. XXXII, No. 1–2, 2002

Absorption of the laser beam during welding with CO_2 laser

JACEK HOFFMAN, ZYGMUNT SZYMAŃSKI

Institute of Fundamental Technological Research, ul. Świętokrzyska 21, 00–049 Warszawa, Poland.

This paper concerns the absorption process of the CO_2 laser beam during laser welding. Both absorption mechanisms, *i.e.*, Fresnel and plasma absorption, are considered. The analysis shows that the Stratton far-infrared approximation fairly well describes the Fresnel absorption of metals near the boiling point. The absorption coefficients for several metals as Fe, Ti, Al and Cu are calculated as a function of temperature. These coefficients are used to calculate the total absorption of the CO_2 laser beam during laser welding of iron and aluminium. The results show the role of specific absorption mechanisms as first Fresnel reflection, multiple reflections and plasma absorption during keyhole welding. Significant differences in the case of iron and aluminium are found in the agreement with experimental observations.

1. Introduction

Growing number of industrial lasers is due to the large field of their technological applications as well as their flexibility. One laser can be used for cutting, welding, drilling, hardening *etc.*, and the time needed to exchange a laser head for the suitable one is less than half an hour. The radiation of a 2–5 kW CO_2 laser can be typically focussed to around 0.2 mm diameter, which means that even at moderate laser power the energy flux density may be equal to several MW/cm^2. This value is comparable to the electron beam energy flux and two orders of magnitude higher than that from an electric arc. It is clear that the laser is the commercial power source with the highest energy flux offered to industry at the present time. The absorption of laser radiation determines the amount of energy transferred to a material and therefore is of deciding importance for a welding process. The knowledge of the absorption coefficients is necessary for proper modelling of the welding process.

The absorption process during welding with CO_2 laser is studied in this paper. Both absorption processes, Fresnel and plasma absorption, are considered. Absorption coefficients for such metals as Fe, Ti, Al and Cu are calculated as a function of temperature. The calculation of the CO_2 laser radiation absorption during laser welding of iron and aluminium is also made showing significant differences in the role of Fresnel and plasma absorption mechanisms in these two cases.

2. Mechanism of a deep welding

If the intensity of laser radiation exceeds 1 MW/cm^2 the recoil force exerted by the evaporating particles on the liquid surface is so strong that it expels the molten material aside. The strongest recoil pressure is exerted in the middle of the laser beam where the beam intensity has a maximum. Such an interaction of intense laser radiation with a workpiece leads to the formation of a long, thin, cylindrical cavity in a metal, called a keyhole. Generation of a keyhole enables the laser beam to penetrate into the workpiece and is essential for a deep welding.

The keyhole contains ionized metal vapour (plasma) and is surrounded by molten material called the weld pool. The temperature of the metal vapour inside a keyhole is 15000–20000 K [1], [2]. To keep a keyhole open the metal vapour pressure p inside a keyhole must be slightly greater than the ambient pressure. The excess of pressure is necessary to balance the surface tension that tends to close the keyhole. The height of the plasma plume is determined by the interaction between the stream of hot metal vapour and the stream of cold shielding gas from the opposite side.

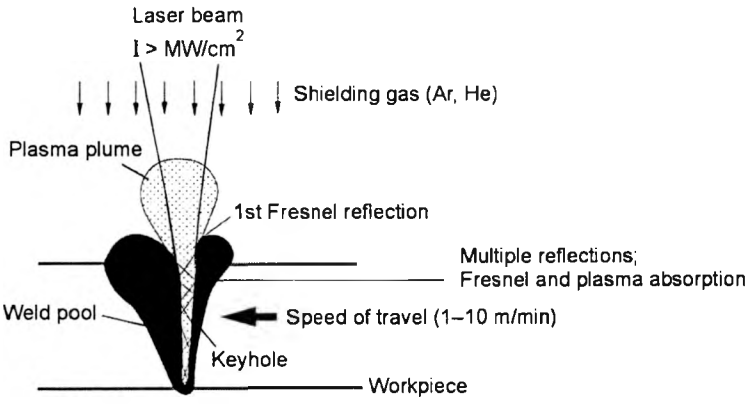

Fig. 1. Mechanism of keyhole welding.

The mechanism of the absorption of the laser beam during welding process is shown schematically in Fig. 1. The laser beam passes through the plasma plume, which absorbs a small part (less than 10%) of the laser power [3]. This part of radiation is lost for the welding process – only small fraction of the absorbed power is transferred back to the surface by plasma radiation and conduction. Next, the transmitted laser radiation falls on the metal surface and during the so-called first Fresnel reflection up to 40% of the remaining laser power is absorbed. Further Fresnel absorption takes place through multiple reflections from the keyhole wall (now the angle of incidence decreases and the absorption is smaller). Between the reflections the radiation is absorbed by the plasma filling the keyhole and subsequently its energy is transferred to the melt. The central part of the laser beam has no contact with the

wall for the most of its way and is absorbed only by the plasma until it reaches the keyhole bottom.

3. Fresnel absorption

The electromagnetic wave that falls on a gas–solid (plasma–metal) interface is partly reflected, partly absorbed and transmitted; the sum of the coefficients equals unity $R + A + T = 1$. Direct absorption of the electromagnetic radiation by the metal surface is called the Fresnel absorption. The ratio of the intensities of the incident and reflected wave is called the reflection coefficient. Since transmission in metals is negligible, $T = 0$ and $A = 1 - R$.

The incident wave is characterized by the angle of incidence θ, between the ray direction and normal to the surface, and polarization P. The metal is characterized by the real and imaginary part of the complex refractive index (n and k, respectively). Therefore $A = A(n, k, \theta, P)$ and $R = R(n, k, \theta, P)$.

In this paper, we consider the electromagnetic wave which is propagated in a medium 1, reaches the boundary of this medium with medium 2 (metal) and reflects from the metal surface. When the medium 1 is vacuum, or an ambient gas or plasma, its refractive index equals unity or is very close to it. Therefore $n_1 = 1$ and the relative index of refraction of the second medium with respect to first one is $n_{12} = n_2/n_1 = n_2$, where indices 1 and 2 denote the ambient gas and metal, respectively.

The temperature of the keyhole wall is close to the boiling temperature. Unfortunately, the data of optical constants of liquid metals at boiling temperature at 1 atm are very scarce. This is connected with the experimental difficulties [4]. To get boiling metal free from impurities very low ambient pressure is needed which reduces strongly the boiling temperature. The (not numerous) measurements of the absorption during welding process do not allow separation of various absorption mechanisms and parameters like angle of incidence, wall temperature, *etc.* The lack of data makes it necessary to rely on approximate methods described below.

The general equation of wave motion obtained from the Maxwell equations for homogeneous medium with no volume charge has the form

$$\nabla^2 \mathbf{E} - \mu\varepsilon \frac{\partial^2 \mathbf{E}}{\partial t^2} - \mu\sigma \frac{\partial \mathbf{E}}{\partial t} = 0 \tag{1}$$

where $\mathbf{E}$ is electric field intensity, and ε, μ and σ are dielectric permittivity, magnetic permeability and conductivity, respectively. Similar equation can be obtained for the magnetic field.

Inserting the expression for the plane wave $\mathbf{E} = \mathbf{E}_0 \exp(i\mathbf{k} \cdot \mathbf{r} - i\omega t)$, where $\mathbf{E}_0$ is the wave amplitude, ω the angular frequency, and $\mathbf{k}$ the wave vector, one gets a dispersion relation

$$|\mathbf{k}|^2 = \omega^2 \varepsilon\mu + i\omega\mu\sigma. \tag{2}$$

In a free space $\varepsilon = \varepsilon_0$, $\mu = \mu_0$ and $\sigma = 0$, so

$$|\mathbf{k}|^2 = \omega^2 \varepsilon_0 \mu_0 = \frac{\omega^2}{c^2} \tag{3}$$

where c is the speed of light in a free space. The angular frequency of the CO_2 laser radiation is 1.78×10^{14} s^{-1}.

The visible and infrared radiation has magnetic permeability $\mu = \mu_0$ in most dielectric and conducting media. In the case of dielectrics $\sigma = 0$ and then

$$|\mathbf{k}|^2 = \omega^2 \varepsilon \mu_0 = \frac{\omega^2}{c^2} n^2 \tag{4}$$

where n is the refractive index whose square is equal to the relative (to a free space) dielectric permittivity

$$n^2 = \varepsilon_1 = \frac{\varepsilon}{\varepsilon_0}. \tag{5}$$

For the conductors

$$|\mathbf{k}|^2 = \frac{\omega^2}{c^2}\left(\frac{\varepsilon}{\varepsilon_0} + i\frac{\sigma}{\varepsilon_0 \omega}\right) = \frac{\omega^2}{c^2}\hat{n}^2. \tag{6}$$

The square of the complex refractive index is

$$\hat{n}^2 = (n + ik)^2 = \varepsilon_1 + i\varepsilon_2 \tag{7}$$

where n and k are real and imaginary part of the refractive index, respectively, and the right hand side of the relation (7) describes the complex dielectric permittivity.

It is easy to notice that the propagation of the electromagnetic wave in a conductive medium differs from that in a dielectric. In conductors both the dielectric permittivity and refractive index are complex quantities that additionally depend on the wave frequency. The extinction coefficient k describes the dumping of the electromagnetic wave in the medium – the wave amplitude decreases e-fold on the path of $(k\omega/c)^{-1}$. In the case of metals, for visible and infrared radiation $k \gg 1$, the wave amplitude decreases on the path much smaller than the wavelength in the vacuum. The thickness of the layer $\delta = c/\omega k$ which is penetrated by the electromagnetic wave is called the skin depth and is of the order of $\sim 10^{-6}$ cm (see values of $1/k = m$ in Tab. 1).

Separating the real and imaginary part of the refractive index we get

$$n^2 - k^2 = \varepsilon_1, \qquad 2nk = \varepsilon_2 \tag{8}$$

or, for n and k

$$n = \sqrt{\frac{1}{2}(\varepsilon_1 + \sqrt{\varepsilon_1^2 + \varepsilon_2^2})}, \qquad k = \sqrt{\frac{1}{2}(-\varepsilon_1 + \sqrt{\varepsilon_1^2 + \varepsilon_2^2})}. \tag{9}$$

Table 1. Electrical conductivity and absorption of 10.6 μm radiation at normal incidence for some metals at room temperature.

Metal	Cu	Al	Fe	Ti
σ_0 [$10^6\ \Omega^{-1}m^{-1}$]	59.8	37.2	10.3	1.82
$m = 1/k$	0.00726	0.00920	0.0175	0.0416
A [%] approximation formula	1.44	1.82	3.44	7.98
A [%] experiment	1.22–1.81 [12]	1.14 [8]	2.25 [8], 2.80 [12]	3.70 [8]

The reflection coefficients are given by the Fresnel equations. Depending on polarization they are [5]

$$R_S(n, k, \theta) = \frac{(a - \cos\theta)^2 + b^2}{(a + \cos\theta)^2 + b^2}, \tag{10}$$

$$R_P(n, k, \theta) = \frac{(a\cos\theta - \sin^2\theta)^2 + b^2\cos^2\theta}{(a\cos\theta + \sin^2\theta)^2 + b^2\cos^2\theta} R_S(n, k, \theta). \tag{11}$$

Indices S and P denote perpendicular and parallel polarization respectively, *i.e.*, the electric vector of the incident beam is either perpendicular or parallel to the plane of incidence and variables a and b are functions of n and k (or ε_1 and ε_2) and angle of incidence θ

$$a = \sqrt{+c + \sqrt{c^2 + n^2k^2}}, \tag{12}$$

$$b = \sqrt{-c + \sqrt{c^2 + n^2k^2}} \tag{13}$$

where

$$c = \frac{1}{2}(n^2 - k^2 - \sin^2\theta). \tag{14}$$

The reflection coefficient for the wave of arbitrary polarization can be obtained from the above formulas. In the case of circularly polarized light the reflection coefficient is the arithmetic mean of R_S and R_P

$$R_C = \frac{1}{2}(R_S + R_P). \tag{15}$$

In the case of normal incidence ($\theta = 0$) the reflection coefficient does not depend on the polarization and is given by

$$R = \frac{(n-1)^2 + k^2}{(n+1)^2 + k^2}, \tag{16}$$

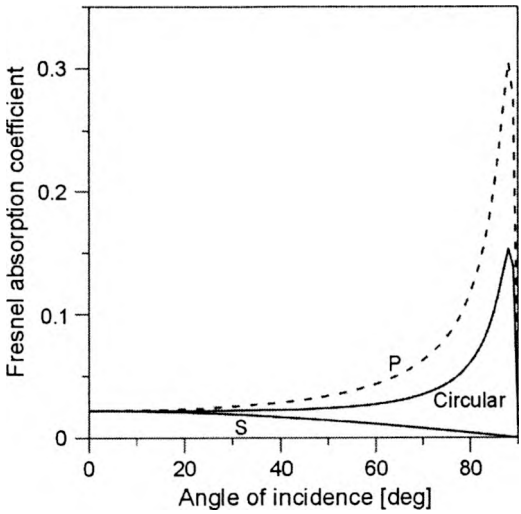

Fig. 2. Fresnel absorption coefficient of polarized CO_2 radiation for iron at room temperature; $n = 5.97$, $k = 32.2$ were taken from [11].

and the absorption coefficient is

$$A = \frac{4n}{(n+1)^2 + k^2}. \tag{17}$$

The optical properties of conductors can be derived from the Drude model. In this model it is assumed that only free electrons move under the action of the electromagnetic field; the much heavier particles like atoms and ions are at rest. The equation of the electron motion has the form

$$\frac{\mathrm{d}^2\mathbf{x}}{\mathrm{d}t^2} + \nu\frac{\mathrm{d}\mathbf{x}}{\mathrm{d}t} = -\frac{e_0}{m_e}\mathbf{E}_0\exp(-i\omega t) \tag{18}$$

where e_0 and m_e are the electron charge and mass, respectively, $\mathbf{E}_0$ is the intensity of the electric field, and ν is total electron collision frequency for momentum exchange. In metals the relevant electron collisions are those with phonons and lattice defects; electron–electron collisions do not dissipate the electric field energy.

The solution is given by a vector

$$\mathbf{x} = \frac{1}{\omega(\omega + i\nu)}\frac{e_0}{m_e}\mathbf{E}_0\exp(-i\omega t). \tag{19}$$

The complex dielectric permittivity is connected with the polarization vector $\mathbf{P} = \mathbf{D} - \varepsilon_0\mathbf{E}$ by the equation

$$\varepsilon\mathbf{E} = \varepsilon_0\mathbf{E} + \mathbf{P} = \varepsilon_0\mathbf{E} - e_0N_e\mathbf{x} \tag{20}$$

where N_e is the electron density. Inserting to the above equation the vector **x**, after some transformations we get formula for the complex dielectric permittivity $\hat{\varepsilon} = \varepsilon/\varepsilon_0$

$$\hat{\varepsilon} = \varepsilon_1 + i\varepsilon_2 = 1 - \frac{\omega_p^2}{\omega^2 + \nu} + i\frac{\omega_p^2 \nu}{(\omega^2 + \nu^2)\omega} \tag{21}$$

where

$$\varepsilon_1 = 1 - \frac{\omega_p^2}{\omega^2 + \nu}, \qquad \varepsilon_1 = 1 - \frac{\omega_p^2}{\omega^2 + \nu}\frac{\nu}{\omega},$$

and the quantity ω_p

$$\omega_p = \sqrt{\frac{e_0^2 N_e}{\varepsilon_0 m_e}} = 56.5\sqrt{N_e}, \qquad [s^{-1}] \tag{22}$$

where N_e is in m^{-3}, describes the oscillation frequency of free electrons and is called the plasma frequency. The optical properties of medium depend not only on the radiation frequency but also on quantities characteristic of the medium–plasma frequency and electron collision frequency.

The current density is

$$\mathbf{j} = \sigma\mathbf{E} = -e_0 N_e \frac{d\mathbf{x}}{dt} \tag{23}$$

and using again the solution of the equation of the electron motion we get formula for the electrical conductivity of the medium

$$\sigma = \frac{\varepsilon_0 \omega_p^2}{\omega^2 + \nu^2}(\nu + i\omega). \tag{24}$$

It should be stressed that the Drude model describes only the interaction of the electromagnetic wave with free electrons, either in plasma or in metals (in this case "free" means electrons in the conduction band). It does not take into account the interaction of the radiation with the bound electrons. The role of the bound-free transitions in plasma or interband transitions in metals increases with the increase in the radiation frequency and in certain cases cannot be neglected (see the next section).

In metals, the electron density $N_e \approx 10^{29}$ m^{-3} which leads to the inequality $\omega_p > \omega$ and $\varepsilon_1 < 0$. This means that metals are opaque to the CO_2 radiation. For determination of the reflection coefficient R (or absorption A), the knowledge of the two characteristic parameters, plasma frequency ω_p and collision frequency ν, is necessary. The electrical conductivity for direct current ($\omega = 0$) equals to

$$\sigma_0 = \frac{\varepsilon_0 \omega_p^2}{\nu}, \tag{25}$$

and therefore it can be used as one of the parameters. Because collision frequency of free electrons with the phonons and lattice defects is difficult to measure, the electrical conductivity together with plasma frequency are used for determination of metal absorption coefficients. If not available the electrical conductivity can be calculated from the thermal conductivity using the Wiedemann–Franz relation.

Unfortunately, the real metal structure is more complicated than that represented by the Drude model. Only for few metals with simple band structure, as aluminium and lead, exist enough data to formulate semiempirical models [6], [7] that correctly, *i.e.*, in agreement with experimental data, describe the optical properties of metal in dependence on radiation frequency and temperature (the last parameter modifies both plasma and collision frequency). In other cases the experimental data of optical constants of metals, n and k, determined by the ellipsometry technique [8] lead to the values of ω_p and ν that give the optical conductivity $\varepsilon_0 \omega_p^2 / \nu$ considerably different than the electrical conductivity σ_0.

In liquid metals, the interband transitions are not observed [9] and it can be expected that the absorption is approximately Drude-like. In [10] Arnold introduced simple expressions which describe the temperature dependence of the optical constants of several metals in the frame of the Drude model. He assumed that plasma frequency is independent of temperature below the melting point and above changes as the square root of the metal density ρ(T)

$$\omega_p^2(T_2) = \omega_p^2(T_1) \frac{\rho(T_2)}{\rho(T_1)}. \tag{26}$$

The collision frequency varies with the temperature like the direct current conductivity of metal (see Eq. (25))

$$\nu(T_2) = \nu(T_1) \frac{\sigma_0(T_1)\rho(T_2)}{\sigma_0(T_2)\rho(T_1)}. \tag{27}$$

These formulas allowed ARNOLD [10] to calculate the optical constants in high temperature from the known data at room temperature. The absorption in the solid and liquid state calculated in this way is in good agreement with the experimental data [10] and more sophisticated model [6].

The fact that the collision frequency increases with the temperature has an important implication. For Al at room temperature the collision frequency $\nu \approx 10^{14}\,\mathrm{s}^{-1}$, while near the boiling point $\nu \approx 10^{15}\,\mathrm{s}^{-1}$. Taking into account dependence of the Drude dielectronic function on collision frequency, it follows from the above considerations that for liquid metals the far-infrared Stratton formula [5] is reasonable approximation also for 10.6 μm. The far-infrared approximation strongly reduces the

number of parameters necessary to calculate the reflection coefficient. For metals at room temperature and for wavelength $\lambda \geqslant 25$ μm it holds [5]

$$\varepsilon_2 \gg |\varepsilon_1| \text{ and } m = \sqrt{\frac{2}{\varepsilon_2}} \cong \sqrt{\frac{2\varepsilon\omega}{\sigma}} \ll 1 \tag{28}$$

The above assumptions hold for a low frequency radiation $\omega \ll \nu$ where ν is the electron collision frequency. The frequency validity range depends on specific metal.

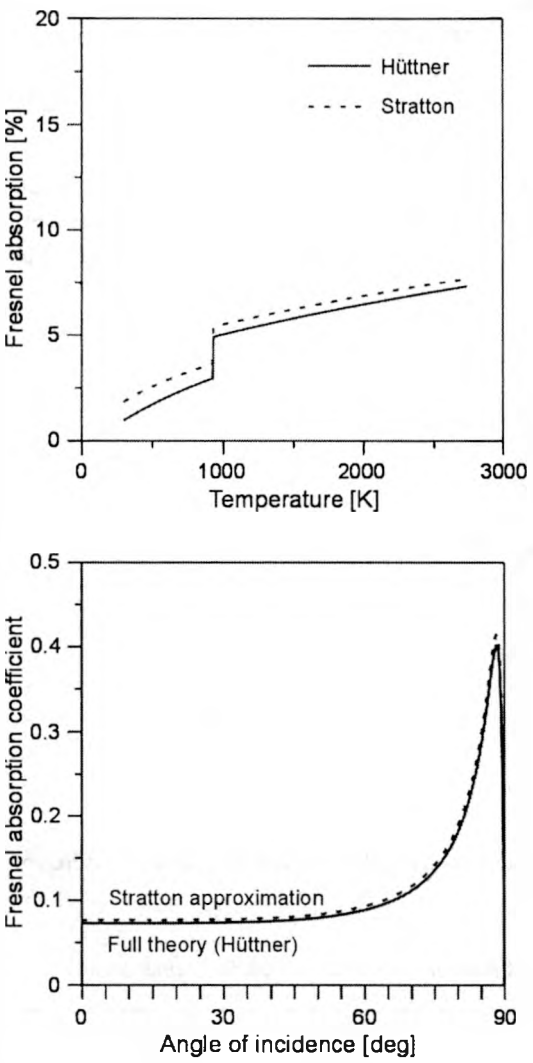

Fig. 3. Fresnel absorption of Al surface at normal incidence as a function of temperature (**a**), Fresnel absorption coefficient of circularly polarized CO_2 radiation for aluminium at boiling temperature (**b**); (—— semiempirical model of Hüttner , – – – Stratton's approximate formula).

Using the above assumptions one gets $n = k = m^{-1}$, $a = b = m^{-1}$. With the accuracy to the quadratic terms of the small parameter m the reflection coefficients are [5]

$$R_S = \frac{1 + (1 - m\cos\theta)^2}{1 + (1 + m\cos\theta)^2}, \tag{29}$$

$$R_P = \frac{\cos^2\theta + (\cos\theta - m)^2}{\cos^2\theta + (\cos\theta + m)^2}. \tag{30}$$

At normal incidence the absorption coefficient is

$$A = \frac{2m}{1 + m + 0.5m^2}. \tag{31}$$

For metals at room temperature and 10.6 μm radiation the discrepancies between experiment and approximate Stratton formula are considerable (see Tab. 1). However, since the ratio ν/ω increases with the temperature it can be expected that the

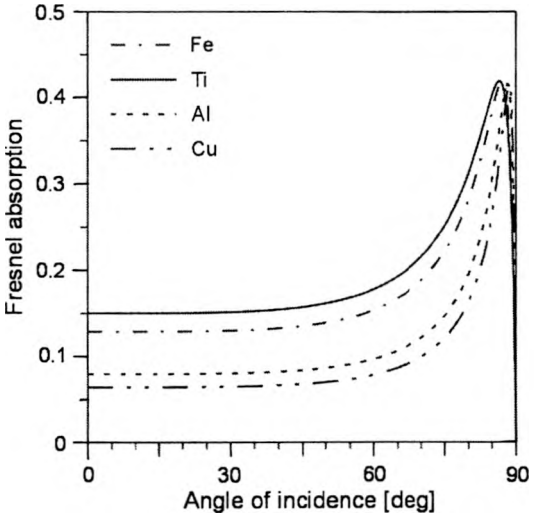

Fig. 4. Fresnel absorption at metal boiling temperature for circularly polarised CO_2 beam for different metals (Stratton formula).

T a b l e 2. Electrical conductivity [13], [14] and factor m for some metals in boiling temperature.

Metal	Al	Ti	Fe	Cu
Boiling temperature [K]	2740	3550	3163	2840
Conductivity [$10^6\ \Omega^{-1}m^{-1}$]	2.0 [13]	0.51 [13]	0.68 [13]	2.89 [14]*
m	0.04	0.08	0.068	0.033

* Calculated from thermal conductivity

conditions (28) are better fulfilled in higher temperatures and for liquid metals the far-infrared approximation holds also at the 10.6 μm wavelength. Indeed, the values of the absorption coefficient calculated for aluminium from the semiempirical model of Hüttner and Stratton approximate formula are very close at boiling temperature (see Figs. 3). At normal incidence the difference between absorption coefficients obtained from both models amounts to 90% at the temperature of 300 K, but it decreases to 5% at the boiling temperature 2740 K (Fig. 3a). Therefore it can be assumed that the far-infrared approximation can be used for other liquid metals. The results of calculations are shown in Fig. 4; the parameters used for calculations are collected in Tab. 2.

4. Plasma absorption

The plasma absorption coefficient can also be calculated from the classical formulas (8), (9) and (21). Since the plasma temperature is about 10000 K and the electron density $N_e \sim 10^{23}$ m^{-3}, total electron collision frequency $\nu \equiv \Sigma\nu$ is much lower than plasma frequency ω_p which in turn is much lower than laser radiation frequency ω; $\nu \ll \omega_p \ll \omega$. From Eqs. (9) and (8) we get then $n = (\varepsilon_1)^{1/2} \approx 1$ and $k = \varepsilon_2/2 \ll 1$. This means that the laser radiation can pass through the plasma and the absorption coefficient κ is related to the extinction coefficient k by the formula $k = 2k\omega/c$. Together with Eq. (21) this leads to the plasma absorption coefficient

$$\kappa = \frac{e_0^2}{\varepsilon_0 mc} N_e \sum_h \frac{\nu_{eh}}{\omega^2 + \nu_{eh}^2} = 1.06 \times 10^{-5} N_e \sum_h \frac{\nu_{eh}}{\omega^2 + \nu_{eh}^2}, \quad [\mathrm{m}^{-1}] \tag{32}$$

where N_e is in m^{-3}, ν_{eh} is the frequency of the electron-heavy-particle collisions and the summation is taken for all types of the collision. Since $\omega^2 \gg (\Sigma\nu_{eh})^2$ the formula (32) can be approximated by

$$\kappa = 1.06 \times 10^{-5} N_e \sum_h \frac{\nu_{eh}}{\omega^2}. \tag{33}$$

The formula (32) is frequently used to calculate the absorption coefficient. The electron–ion collision frequency is given by [15]

$$\nu_{ei} = 3.64 \times 10^{-6} T^{-3/2} \sum_i z^2 N_i \ln\Lambda, \tag{34}$$

where $\ln\Lambda$ is so-called Coulomb-logarithm with Λ [15]

$$\Lambda = 1.24 \times 10^7 z^{-1} T^{3/2} N_e^{-1/2} \tag{35}$$

and N_i is the ion density (in m^{-3}), T is the temperature (in kelvins), and z is the particle charge. Equation (34) is obtained from the energy-averaged Coulomb cross-section

and is limited by the condition $\ln\Lambda \gg 1$. Since in the case of the metal plasma $\ln\Lambda \sim 3$ in the large region of plasma parameters $\ln\Lambda$ in Eq. (33) should be replaced by $\ln\Lambda - 1.37$ [15].

Although the classical electrodynamics formula (32) is often used for calculation of the plasma absorption coefficient it is preferred to use formulation from the atomic physics. The reason is that formula (32) does not include another important absorption process, namely the photoionization. The importance of this process will be discussed below.

The absorption of the radiation in plasma can be described by the absorption coefficient [16]

$$\kappa_\lambda = \kappa_\lambda^{fb} + \kappa_\lambda^{ff} = \sum_{E_i}^{0} N_E^z \sigma_E(\lambda) + \sum_{E_i}^{-\infty} N_E^z \sigma_E(\lambda) \tag{36}$$

where indexes *fb* and *ff* denote free-bound and free-free transition, *i.e.*, absorption of the radiation in the process of photoionization and inverse Bremsstrahlung, respectively. N_E^z is the atom (ion) density in the quantum state with the energy E and $\sigma_E(\lambda)$ is the cross-section for photon absorption. The summation in the first term is taken over all bound states with the ionization energy E_i smaller than the photon energy. In the second term the summation is over all unbounded states with the ionization energy between zero and minus infinity which represent free electrons with the Maxwellian energy distribution [16]. The cross-section $\sigma_E(\lambda)$ is usually given in the form $\sigma_E^{cl}(\lambda)G$, where $\sigma_E^{cl}(\lambda)$ is the classical cross-section for photon absorption and the Gaunt factor G is the quantum-mechanical correction to the classical cross -section; G_{ff} for free-free and G_{fb} for free-bound transitions).

After calculations the plasma absorption coefficient is given by [17]

$$\kappa = \left\{ C\lambda^3 N_e T^{-1/2} \sum_z z^2 N_z \left[\left(\exp\left(\frac{h\nu}{kT}\right) - 1 \right) \frac{g_z}{U_z(T)} G_{fb} + G_{ff} \right] + \kappa_{ea} \right\}$$

$$\times \left[1 - \exp\left(-\frac{h\nu}{kT}\right) \right] \tag{37}$$

where $C = 1.3674 \times 10^{-27}$ in MKS units. The first bracket contains the absorption due to the photoionization and electron-ion inverse Bremsstrahlung [17] and κ_{ea} denotes absorption due to the electron-atom inverse Bremsstrahlung. The last bracket contains contribution from the stimulated emission. N_e and N_z are electron and ion density in m^{-3}, respectively, T – temperature in kelvins, z denotes ionization stage, $U_z(T)$ partition function, and E_z ionization energy. The factor $g_z/U_z(T)$, where g_z is the statistical weight of the parent ion, appears in more rigorous formulations [18] but the value of the absorption coefficient does not change significantly if g_z is replaced by

$U_z(T)$ and the factor $g_z/U_z(T)$ reduces to unity. The Gaunt factors are of order unity; $G_{fb} = 1$ can be assumed and $G_{ff} = 1.2–1.3$ [19]. The photoionization formula has been derived for hydrogen-like atoms but in the case of 10.6 μm (or 1.06 μm) radiation the corrections for complex atoms should be negligible because the photoionization takes place from highly excited states which tend to follow the hydrogen level structure.

The absorption due to the electron–atom collisions does not exceed few per cent of the total absorption in the temperature region of interest. The formula (37) is valid for radiation frequencies larger than plasma frequency ω_p, otherwise the absorption coefficient scales as $\kappa = \kappa(1 - \omega_p^2/\omega^2)^{-1/2}$ [20].

It is clear from relation (37) that the relative contribution of the photoionization and inverse Bremsstrahlung to the absorption coefficient is like $[\exp(h\nu/kT)-1]$ to 1 (assuming $g_z/U_z(T)G_{fb}$ and G_{ff} equal unity). In the case of CO_2 laser radiation at 10.6 μm these contributions are like 0.145:1 (for the temperature of 10000 K) and in the case of Nd:YAG laser radiation at 1.06 μm like 2.89:1. This means that the photoionization process cannot be neglected, especially for wavelengths shorter than 10.6 μm. Since the electrodynamics formula (32) does not take into account this quantum phenomenon therefore, in this work we use relation (37) for calculations of the absorption coefficient.

The coefficient of the electron–atom inverse Bremsstrahlung can be calculated using the approximate expression [21] for the emission coefficient

$$\varepsilon_{ea,\nu} = \frac{16e^2}{3\varepsilon_0 c^3}\left(\frac{k}{2\pi m}\right)^{3/2} N_a N_e T^{3/2} Q(T) \tag{38}$$

where N_a is atom density and $Q(T)$ is the average electron–atom impact cross-section.

From the Kirchhoff's law

$$\varepsilon_\nu = \kappa'(\nu) B_\nu(T) \tag{39}$$

where and $B_\nu(T)$ is the intensity of the black body radiation we get an expression for the absorption due to the electron–atom inverse Bremsstrahlung

$$\kappa'_{ea}(\nu) = \frac{4e^2}{3\varepsilon_0 mc}\frac{N_e \nu_{ea}}{\omega^2} = 1.41 \times 10^{-5}\frac{N_e \nu_{ea}}{\omega^2}, \quad [\mathrm{m}^{-1}] \tag{40}$$

where $\omega = 2\pi\nu$ is the laser radiation frequency, and

$$\nu_{ea} = \left(\frac{8kT}{\pi m_e}\right)^{1/2} Q(T) N_a \tag{41}$$

is the frequency of electron–atom collisions.

It is worth noting that the formula (40) and formula (33) give quite similar results for κ_{ea} – the absorption coefficient due to the electron–atom inverse Bremsstrahlung.

The absorption coefficient can be calculated provided the plasma composition is known. It can be assumed [3] that the plasma induced during laser welding is in the state of local thermal equilibrium (LTE). LTE means that energy states of the particles are populated as in complete thermal equilibrium, but the accompanying blackbody radiation field is reduced. All energy distributions, with the exception of Planck's radiation law, obey equilibrium relationship.

In LTE the ratio of the densities of particles in two consecutive ionization stages is given by the Saha equation [17]

$$N_e \frac{N_z}{N_{z-1}} = 2\frac{U_z(T)}{U_{z-1}(T)} \frac{(2\pi m_e kT)^{1/2}}{h^3} \exp\left(-\frac{E_{z-1} - \Delta E_{z-1}}{kT}\right) \tag{42}$$

where N_{z-1} and N_z are particle densities (z denotes ionization stage, $z = 1$ for neutral atoms), $U_{z-1}(T)$ and $U_z(T)$ are partition functions, m_e is the electron mass, and $\Delta E_{i,\,z-1}$ – the lowering of the ionization energy. For metals the partition functions can be found in [22]–[24].

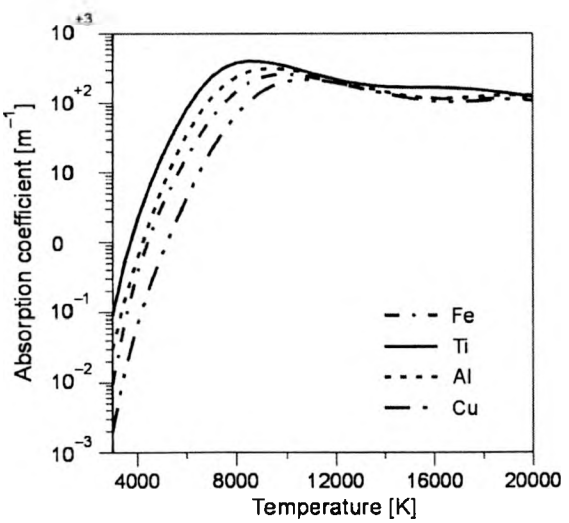

Fig. 5. Plasma absorption coefficient (LTE, 1 atm pressure) for different metals.

Together with the Dalton law and the condition of electrical neutrality the Saha equation can be used to determine the plasma composition inside the keyhole at a given temperature T. Such calculations have been made and the plasma absorption coefficient for various metals is subsequently calculated from the relation (37). The results are shown in Fig. 5.

The frequency of electron–Fe atom collisions is $\nu_{ea}^{Fe}/N_a = 9.26 \times 10^{-13}\ \mathrm{m^3 s^{-1}}$ was taken from [25]. The contribution of electron–atom inverse Bremsstrahlung to the total absorption coefficient is significant in low temperatures, in the case of Fe

plasma, for $T < 7000$ K. In higher temperatures it is negligible. For aluminium $\nu_{ea}^{Al}/N_a = 2.1 \times 10^{-13}$ m^{3}s^{-1} was taken from [26]. For copper the electron–atom collision frequency was calculated from the relation (41). The cross-section $Q(T)$ was estimated from the cross-section data given in [27] assuming $Q(T) \sim T^{-1/2}$ relationship. This gave collision frequency $\nu_{ea}^{Cu}/N_a = 2.35 \times 10^{-13}$ m^{3}s^{-1}. The frequency of electron–atom collisions for titanium has been assumed similar to that for iron.

In the case of 10.6 μm radiation the absorption coefficient obtained from the formula (32) is about 25% smaller than that obtained from the formula (37). If Coulomb-logarithm is not diminished by subtraction of the factor 1.37 the formula (32) gives the values of the absorption coefficient about 25% higher than the formula (37).

5. Calculations of the absorption inside the keyhole

The relative importance of both absorption mechanisms, the Fresnel and plasma absorption, can be checked by changing the polarization of the laser beam [28]. Since the Fresnel absorption depends strongly on polarization, the welding depth increases considerably when the laser beam is *P*-polarized. In fact this effect is observed for the majority of materials when the welding speed is higher than some meters per minute, indicating that the Fresnel absorption is dominant. However, for some materials, like aluminium, the effect of changing polarization of the laser beam is almost negligible [29] showing the importance of the plasma absorption. Therefore the calculations were made for iron and aluminium in order to explain experimental observations.

The detailed results of the calculation of the laser beam absorption in the keyhole are given below. The analysis was based on the ray tracing of the laser beam with Gaussian intensity distribution in the conical, 2 mm deep keyhole, closed at the bottom with upper radius of 0.2 mm and lower radius of 0.06 mm. The laser beam was divided

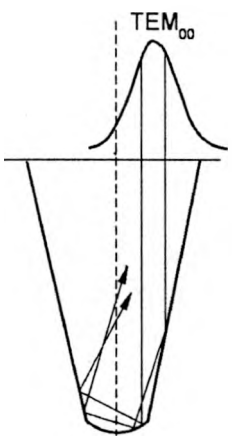

Fig. 6. Schematic representation of the interaction of the laser beam TEM_{00} with the keyhole wall used for the calculation of the absorption.

into 200 rays along the radial direction and the path of each ray was traced according to the geometrical optics. The laser intensity distribution was assumed to be TEM_{00} mode, and exact power was ascribed to each elementary ray. The geometry of the keyhole and the laser beam is shown in Fig. 6. The laser beam falls on the front keyhole wall only, the rear wall is maintained by multiple Fresnel reflections and plasma absorption. According to calculations [30] it has been assumed that the plasma temperature is 20000 K, at the centre of the keyhole and equals to the metal boiling temperature at the wall. In the case of a mild steel 57% of the laser power is absorbed by the Fresnel absorption (31% in the first reflection and 26% in the multiple reflections), 25% is absorbed by the plasma inside the keyhole and the remaining 18% leaves the keyhole back. In the case of aluminium, Fresnel absorption amounts to 44% and plasma absorption to 30% of the laser power; 26% leaves the keyhole. It is worth noting that the ratio of the efficiencies of the two absorption mechanisms, Fresnel and plasma absorption, is considerably different in both above-mentioned cases and equals 2 and 0.88 in the case of iron, and aluminium, respectively.

It should be noted that the calculations concern only the part of the laser radiation which enters the keyhole. The radiation contained in the wings of the intensity distribution is not intense enough to melt the material and is reflected from the surface. This part is different for different materials and amounts to 6–10% and 10–27% in the case of steel and aluminium, respectively depending on the laser power and welding velocity [29].

6. Summary

The analysis shows that the Stratton far-infrared approximation fairly well describes the Fresnel absorption of metals near the boiling point. The absorption coefficients for several metals as Fe, Ti, Al and Cu are calculated as a function of temperature. At the metal boiling temperature the Fresnel absorption coefficients for circularly polarized beam differ significantly for various metals, especially for angles of incidence lower than 75 degrees. Similarly, plasma absorption coefficients are different for various metals for temperatures lower than 10000 K. Calculations of the total absorption during keyhole welding of iron and aluminium show significant differences in the role of plasma and Fresnel absorption, in the case of both metals. This result is in agreement with the experimental observations.

The comparison of the calculated absorption with the experiment is rather difficult because experimental data are scarce. However, in the case of iron the calculated total absorption agrees well (within 10%) with the experimental results obtained for mild steel [31].

References

[1] TIX C., SIMONG., Phys. Rev. E **50** (1994), 453.

[2] DUCHARME R., WILLIAMS K., KAPADIA P., DOWDEN J., STEEN B., GŁOWACKI M., J. Phys. D: Appl. Phys. **27** (1994), 1619.

[3] SZYMAŃSKI Z., KURZYNA J., KALITA W., J. Phys. D: Appl. Phys. **30** (1997), 3153.
[4] BRÜCKNER M., SCHÄFER J.H., UHLENBUSCH J., J. Appl. Phys. **66** (1989), 1326.
[5] STRATTON J.A., *Electromagnetic Theory*, McGraw-Hill, New York, London 1941.
[6] HÜTTNER B., J. Phys. Condens. Matter **6** (1994), 2459.
[7] HÜTTNER B., J. Phys. Condens. Matter **7** (1995), 907.
[8] PALIK E.D. [Ed.], *Handbook of Optical Constants of Solids*, Academic Press, San Diego 1998.
[9] SMITH D.Y., SHILES E., INOKUTI M., *The optical properties of metallic aluminum* [In] *Handbook of Optical Constants of Solids*, [Ed.] E.D.Palik, Academic Press, San Diego 1998.
[10] ARNOLD G.S., Appl. Opt. **23** (1984), 1434.
[11] KIKOIN I.K., *Tables of Physical Constants* (in Russian), [Ed.] Atomizdat, Moscow 1976.
[12] ORDAL M.A., LONG L.L., BELL R.J., BELL S.E., BELL R.R., ALEXANDER R.W., WARD C.A., Appl. Opt. **22** (1983), 1099.
[13] DYOS G.T., FARRELL T. [Eds], *Electrical Resistivity Handbook*, IEE Books, London 1992.
[14] GŁOWACKI M., *Welding of metals with c.w. lasers*, Ph.D.Thesis, University of Essex, Department of Physics, 1994.
[15] MITCHNER M., KRUGER CH.H., Jr., *Partially Ionized Gases*, Wiley, New York, London 1973.
[16] ZELDOVICH JA.B., RAIZER JU.P., *Physics of Shock Waves and High Temperature Hydrodynamic Phenomena*, (Russian edition), Moscow 1963.
[17] RICHTER J., [In] *Plasma Diagnostics*, [Ed.] W. Lochte-Holtgreven, North Holland Pub. Co., Amsterdam 1968.
[18] SCHLÜTER D., Z. Phys., **210** (1968), 80.
[19] WHEELER C.B., FIELDING S.J., Plasma Phys. **12** (1970), 551.
[20] GRIEM H., *Plasma Spectroscopy*, Mc Graw-Hill Book Company, New York 1964.
[21] CABANNES F., CHAPELLE J.C., *Reactions Under Plasma Conditions*, [Ed.] M. Venugopalan, Wiley, New York 1971.
[22] DRAWIN H.W., FELENBOK P., *Data for Plasmas in Local Thermodynamic Equilibrium*, Gauthier -Villars, Paris 1965.
[23] HALENKA J., GRABOWSKI B., Astron. Astrophys. Suppl. Ser. **57** (1984), 43.
[24] HALENKA J., Astron. Astrophys. Suppl. Ser. **75** (1988), 47.
[25] TIX C., SIMON G., J. Phys. D:, Appl. Phys. **26** (1993), 2066.
[26] WEYL G., PIRRI A., ROOT R., AIAA J. **19** (1981), 460.
[27] CHERVY B., DUPONT O., GLEIZES A., KŘENEK P., J. Phys. D: Appl. Phys. **28** (1995), 2060.
[28] BEYER E., *Schweissen mit Laser: Grundlagen*, Springer-Verlag, Berlin, Heidelberg, New York 1995.
[29] SATO S., TAKAHASHI K., MEHMETLI B., J. Appl. Phys. **79** (1996), 8917.
[30] HOFFMAN J., *Laser beam-keyhole interaction during laser welding*, (in Polish), Ph.D.Thesis, Institute of Fundamental Technological Research, Warsaw 2000.
[31] BEYER E., BEHLER K., PETSCHKE U., SOKOLOWSKI W., ROSEN H.G., HAMANN CH., Laser Optoelektron. **18** (1986), 35.

Received November 11, 2001
in revised form March 16, 2002